Analysis of the $t\bar{t}$ Cross Section in the Dielectron Channel

Joseph Kozminski, Robert Kehoe, Harry Weerts
Michigan State University, East Lansing, MI 48824

DØ Note 4196

Draft 1.2

Abstract

We present an analysis of the $t\bar{t}$ cross section in the dielectron channel in 107.0 pb^{-1} of data collected by the DØ detector in Run II.

1 Introduction

In this note, we discuss a preliminary measurement of the top quark cross section times branching ratio in the dielectron channel. Top quark pairs can be produced via $q\overline{q}$ annihilation or gluon fusion. At the Tevatron center-of-mass energy ($\sqrt{s}$ = 1.96 TeV), it is more likely for most of the proton and anti-proton momenta to be carried by one of their constituant quarks than by the gluons; hence, $q\overline{q}$ annihilation is the primary production channel. Nearly 100% of the time, each top decays to a b quark and a W boson in the Standard Model. The $W \to e\nu_e$ branching fraction is 1/9. Thus, the $t\bar{t} \to ee$ branching fraction is 1/81, leading to relatively few $t\bar{t}$ pairs decaying to the dielectron channel.

Even though the branching fraction is small for this channel, there are few background processes with two isolated, high p_T electrons in the final state. Specifically, the experimental signature for the dielectron decay of the top is two isolated, high p_T electrons, two high p_T jets from the b quarks, and large $\not\!\!E_T$ from the two neutrinos. The primary backgrounds for this signature are:

- $Z \to \tau\tau$: The Z cross section is large, but the τ's have a small branching ratio to electrons. Also, the electron p_T spectrum is softer than that of electrons in $Z \to ee$ decays, and there tends to be less $\not\!\!E_T$ than in background processes involving W's.

- $WW \to ee$: The WW production cross section is small, but these events are very top-like in electron p_T and $\not\!\!E_T$. Requiring two jets minimizes this process's contribution significantly.

- Heavy flavor QCD production: The $c\bar{c}$ and $b\bar{b}$ cross section are very large, but electrons from these decays are typically soft and non-isolated. There also tends to be little $\not\!\!E_T$.
- $Z/\gamma^* \rightarrow ee$ This process has a large cross section with two high p_T electrons but no significant $\not\!\!E_T$. Also, the Z mass peak can be resolved.
- $W + jets$: This process has a large cross section, but a high p_T jet has to to fake an isolated electron.
- QCD multijet: The cross section for this is huge. However, two high p_T jets must fake isolated electrons, and these events have no significant $\not\!\!E_T$.

The first three processes comprise the physics background while $Z/\gamma^* \rightarrow ee$, W+jets, and QCD multijet processes make up the instrumental (fake) background.

2 Data Set

2.1 Triggering

The dielectron analysis selects events passing the 2EM_HI trigger. This trigger requires two Level 1 (L1) electromagnetic (EM) towers with $p_T \geq 10$ GeV. At Level 3 (L3), one loose EM object defined as an object with EM fraction> 0.9 in a cone of radius 0.25; however, the p_T cut on the EM object varies by Trigger List. Trigger Lists prior to 9.0 ($runnum < 167019$) require that it have $p_T \geq 10$ GeV. Trigger Lists 9.0 and higher require an EM object with $p_T \geq 20$ GeV. This L3 selection imposes no isolation or shower shape cuts.

The trigger efficiencies have been determined using the data. In order to measure the L1 trigger efficiency, an unbiased data set in which all events pass a muon-only trigger and have an offline reconstructed electron is used. The trigger efficiency is determined by matching the offline electron to a L1 EM trigger tower in a $\Delta R = \sqrt{(\Delta\eta)^2 + (\Delta\varphi)^2} < 0.4$ cone as a function of p_T. The L1 efficiency curve plateaus at 20 GeV with an efficiency of 0.952 ± 0.015.

The L3 trigger efficiency is measured using an unbiased data set comprised of 2EM_HI L3 Mark and Pass events. These are prescaled events which pass the 2EM_HI term at L1 and are recorded regardless of whether they pass the L3 requirement. These L3 EM objects are matched to L1 EM towers and offline electrons in a $\Delta R < 0.4$ cone as a function of p_T in order to determine the L3 trigger efficiency. This efficiency curve becomes fully efficient at 18 GeV for the 10 GeV L3 trigger condition. For the 20 GeV trigger condition, it becomes fully efficient at 27 GeV.

Given an offline cut of $p_T > 20$ GeV, a flat event efficiency of 0.905 ± 0.029 can be applied for runs prior to run 167019. However, for more recent runs, the measured turn-on curve in Figure 1 should be folded into the MC samples to calculate the trigger efficiency. However, when this exercise is performed on the $t\bar{t} \rightarrow ee$ MC sample, the effect is about 0.6%. Hence, the flat efficiency is used, and the effect of the trigger change is accounted for in the 5% systematic on the trigger.

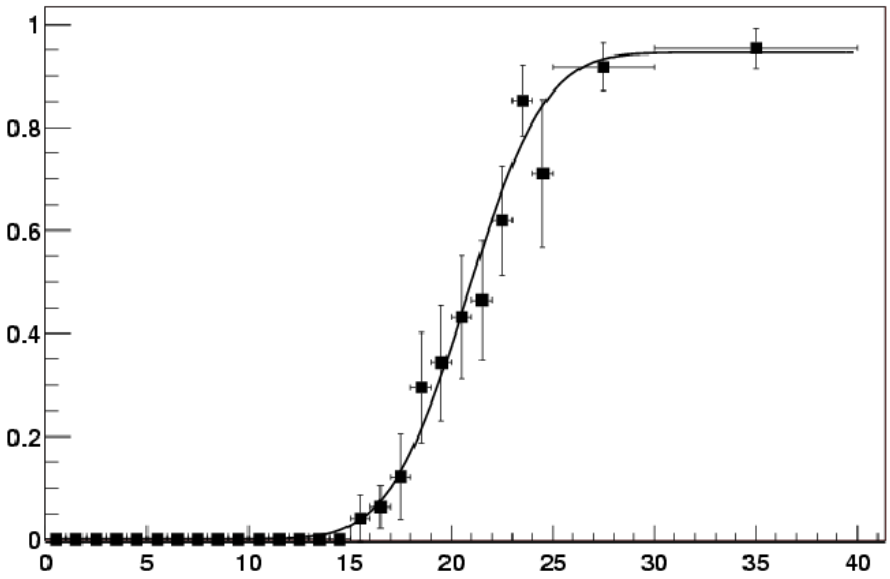

Figure 1: $L1 * L3$ turn-on curve as a function of electron P_T.

2.2 Integrated Luminosity

This analysis utilizes a data sample taken between August 15, 2002 and June 30, 2003. This corresponds to a run range of 161972-178514 and a recorded luminosity of 107.0 pb^{-1} using only good runs. A 10% systematic error on the luminosity is assumed.

The first portion of this run range (to run 174900) employed a Level 1 Calorimeter trigger with coverage extending to $|\eta| < 2.4$. Full coverage to $|\eta| < 3.2$ has been available since then. The run ranges 172359 to 176313 and 177311 to 177925 harbor a problem with less than 4% of the calorimeter channels in which energy was shared across cells due to a problem on specific BLS backplanes. The standard cell-level correction provided by the calorimeter group has been used for this problem. Furthermore, any runs flagged as bad by the SMT, CFT, and Calorimeter detector groups in the Run Quality Database are removed.

The list of good runs produced by the Jet/$\not\!\!E_T$ group is also used in this analysis.The selection criteria for good runs can be found in [1].Finally, in order to use the highest quality data set possible, a small number of luminosity blocks in otherwise good runs are rejected. These luminosity blocks show deviations from quality cuts listed in [2].

2.3 Offline Skimming

The top group has skimmed all of the thumbnails from this data set into several inclusive skims. This analysis uses the "DiEM" skim which requires that events have two EM objects with an uncorrected $p_T \geq 12$ GeV and a particle ID of 10 or 11; 10 being an isolated EM cluster without

an associated track and 11 being an isolated EM cluster with an associated track.

top_analyze $v00-04-02-br06$ is a further skimming tool which applies jet, EM, and $\not\!\!E_T$ corrections; applies identification and quality cuts; and stores the events passing these cuts in a root-tuple format. The jet and $\not\!\!E_T$ corrections are calculated using *jetcorr* $v04-02-03$. Currently, *jetcorr* is used in *top_analyze* to correct all jets passing the quality cuts listed in Section 4 though it is currently only certified for jets with $p_T > 15$ GeV and $|\eta_j| < 2.5$. The EM corrections are applied by *em_util* $v00-02-80$, *emcandidate* $v00-01-06$, *em_evt* $v00-15-33$, *hmreco* $v00-06-13$, and *emreco* $v00-12-24$.

3 Electron Identification

In order to distinguish electrons from jets, we require electron candidates to pass the following criteria:

- $abs(ID) = 10$ or 11
- $EMfraction > 0.9$
- $EMisolation < 0.15$
- $H-matrix\ \chi^2 < 20$

The efficiency for an id 10 or 11 object, a loose EM object, to pass the EM fraction, EM isolation, and H-matrix χ^2 is 0.877 ± 0.007 [3]. There is a 5% systematic on the electron identification.

To substantially reduce the heavy flavor and Drell-Yan backgrounds, we also apply the following kinematic cuts:

- $p_T > 15$ GeV
- $|\eta| < 1.1$

Some work has been done in attempting to add the calorimeter endcaps (EC) into the analysis; however, the fake rates in the EC are high and not fully understood yet. In order to keep the fake background at a reasonable level, this region of the detector is not currently used.

In addition, a likelihood cut, introduced in [4], is now used instead of a track match. The likelihood includes six parameters:

- $\chi^2_{spatial}$
- $H-matrix\ \chi^2$
- E_T/p_T
- EM Fraction

- Distance of Closest Approach (DCA)
- Track Isolation

Using these parameters in a likelihood discriminates electrons from fakes better than a track match or several square cuts. The likelihood is required to be greater than 0.4. The efficiency for this cut is 0.722 ± 0.008 [3]. The systematics for this cut are broken up with the systematic for the track match determined separately . The systematic uncertainty on the track is 3.2% while the systematic on the likelihood is 5.2%.

Finally, the two electrons are required to have opposite charge. The efficiency for this cut is calculated from a Z sample in data, in which both electrons pass all of the above selection cuts. The efficiency is obtained by dividing the number of events with oppositely-charged electrons by the total number of events in the sample. The efficiency for this cut is 0.988 ± 0.003.

4 Jet Identification

Jets are reconstructed using an *improved legacy cone* algorithm [5] with cone radius $\Delta R = 0.5$ in eta-phi space. Jet-finding is re-run at the thumbnail level in *top_analyze* and coarse hadronic (CH) layers are omitted in seeding. Jets are required to be separated from the nearest electron by $\Delta R_{jet-elec} > 0.5$. Also, jets must pass the following quality cuts defined in v2.1 of the jet ID certification [6]:

- $0.05 \leq EMfraction \leq 0.95$
- $Hot\ fraction < 10.0$
- $n90 > 1$
- $Coarse\ hadronic\ fraction\ (CHF) < 0.4$
- p_T-based cut:
  - if jet $p_T < 25$ GeV: $f90 < 0.7 - 0.5 * CHF$ or $CHF < 0.025$
  - if jet $p_T > 25$ GeV: $f90 < 0.8 - 0.5 * CHF$ or $CHF < 0.05$

where $f90 = n90/nitm$ and $nitm$ is the total number of towers in a jet. This last cut is used to remove fake jets which come from noise in the calorimeter. The cut used here is tighter than the standard cut and was developed in the top group for additional fake jet rejection power [1]. A $^{+5.6}_{-5.3}$ systematic is applied to the jet-energy scale while there is a 8.0% systematic on the jet resolution and a 1.4% systematic on jet ID.

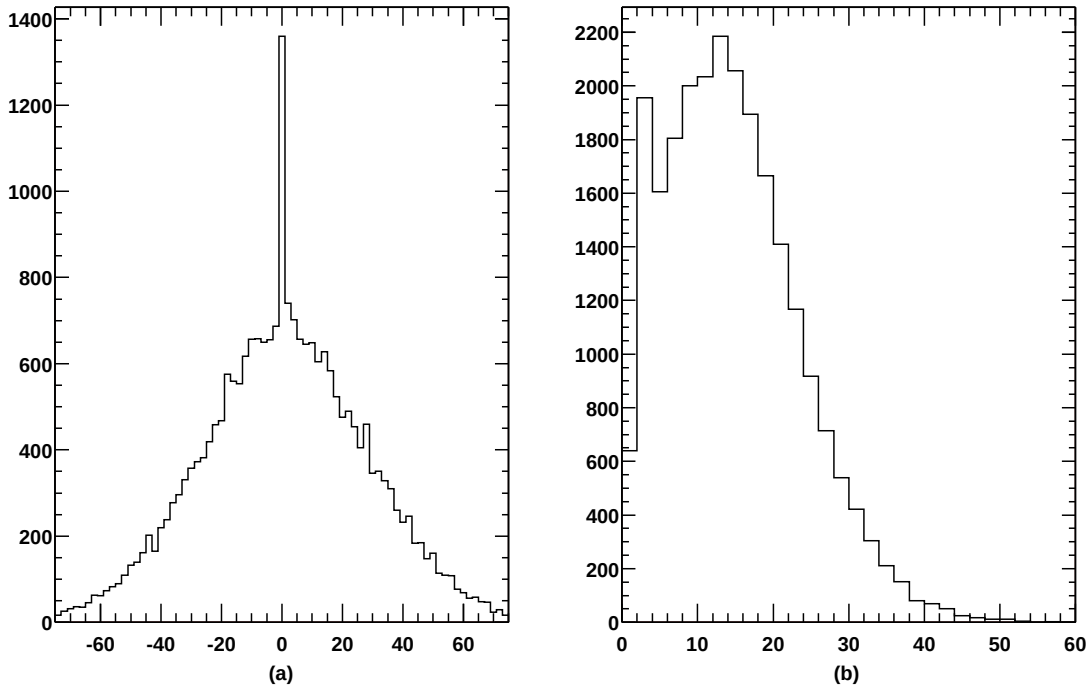

Figure 2: (a) z distribution for the primary vertex and (b) the number of tracks pointing to the primary vertex in a loose-loose diEM sample.

5 Vertexing

Events are required to have a reconstructed vertex with at least three tracks pointing to it using the improved primary vertex algorithm discussed in [7]. In addition, the vertex position along the beamline must be within 60 cm of the center of the detector. The distributions for the vertex position, z, and the number of tracks forming the vertex are shown in Figure 2. The $\not\!\!E_T$ distributions for events with (a) less than three tracks and with (b) three or more tracks making up the vertex is shown in Figure 3. The distribution with fewer than three tracks is clearly wider. This indicates that the $\not\!\!E_T$ resolution is worse for the events in which no vertex is found or only two tracks form the vertex; thus, it is desirable to remove these events. The efficiency for this selection is found in terms of jet multiplicity by dividing the number of events that pass the cuts by the total number of events in the jet bin. These efficiencies can be found in Table 1. The systematic uncertainty for the vertex cuts is 2.0%.

Also, the vertices from which the electrons originate must be within 5 cm of each other along the beam line in order to reject most events in which the electrons originate from different vertices. For top events this cut is nearly 100% efficient. Figure 4 shows $|\Delta z|$ for tight electrons

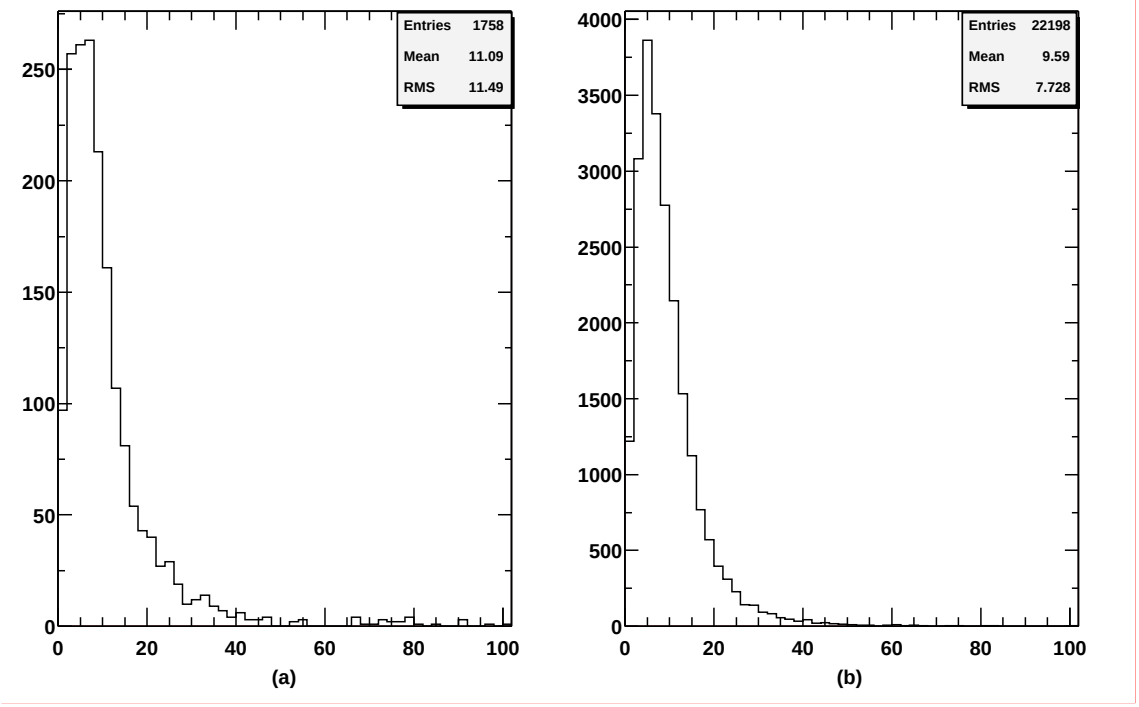

Figure 3: $\not\!\!E_T$ for events with (a) fewer than three tracks and (b) three or more tracks making up the vertex. (c) is the overlay of these plots with (a) normalized to (b).

# of Jets	Efficiency
0	0.937±0.005
1	0.982±0.006
≥2	0.978±0.013

Table 1: Efficiencies for vertex cut with respect to jet multiplicity.

in data and $t\bar{t}\rightarrow ee$ Monte Carlo.

6 Event Selection and Efficiencies

In addition to the identification cuts listed in Section 3, the p_T cut on the electrons is tightened to $p_T > 20$ GeV for additional background rejection.

Cutting on the $\not\!\!E_T$ vs dielectron invariant mass (M_{ee}) distribution is a powerful way to

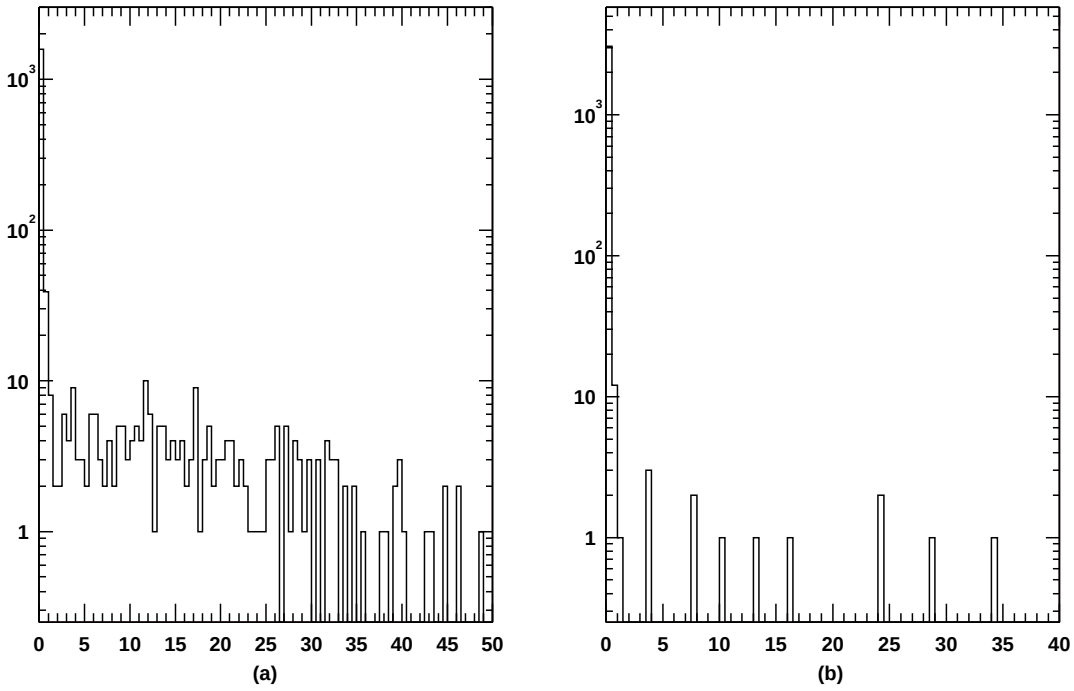

Figure 4: $|\Delta z|$ for tight electrons in (a) data and (b) $t\bar{t}\rightarrow ee$ Monte Carlo.

remove the $Z \rightarrow ee$ background as is evident in Figure 5. This analysis removes events in the Z mass window, which extends from 75 GeV $< M_{ee} <$ 105 GeV, and requires at least 25 GeV of $\not\!\!E_T$ in all other events.

Because of the kinematic distribution of jets in top events, only jets within $|\eta| < 2.5$ are selected. Also, to further reject background, the jets are required to have $p_T > 20$ GeV. Finally, an $H_T^e = p_T^{e1} + p_T^{j1} + p_T^{j2}$ cut of $H_T^e > 120$ GeV is applied in order to gain even more discrimination between signal and background.

The efficiencies for the kinematic cuts, as well as the acceptance and reconstruction efficiencies, are obtained from p13.08.00 $t\bar{t}\rightarrow ee$ Monte Carlo (MC) generated using Pythia with the CTEQ4L PDF set. These efficiencies can be found in Table 2. The electron ID and the likelihood cuts are applied in the MC. The efficiency for these cuts are found in the MC; then, $\kappa = \epsilon_{data}/\epsilon_{MC}$ can be defined in order to relate the MC and data efficiencies. Multiplying the overall efficiency in Table 2 by the κ factors in Table 3 and all of the other calculated efficiencies gives a total signal efficiency of $\epsilon_{top} = 0.063 \pm 0.014$, which corresponds to an expected event yield of 0.62 ± 0.14 events.

Of course, no cut is made to remove the contributions from $t\bar{t}\rightarrow e\tau \rightarrow ee$ and $t\bar{t}\rightarrow \tau\tau \rightarrow ee$. Hence a correction factor, C_τ, for this contribution has been obtained from p14.02.00 $t\bar{t}\rightarrow ll$

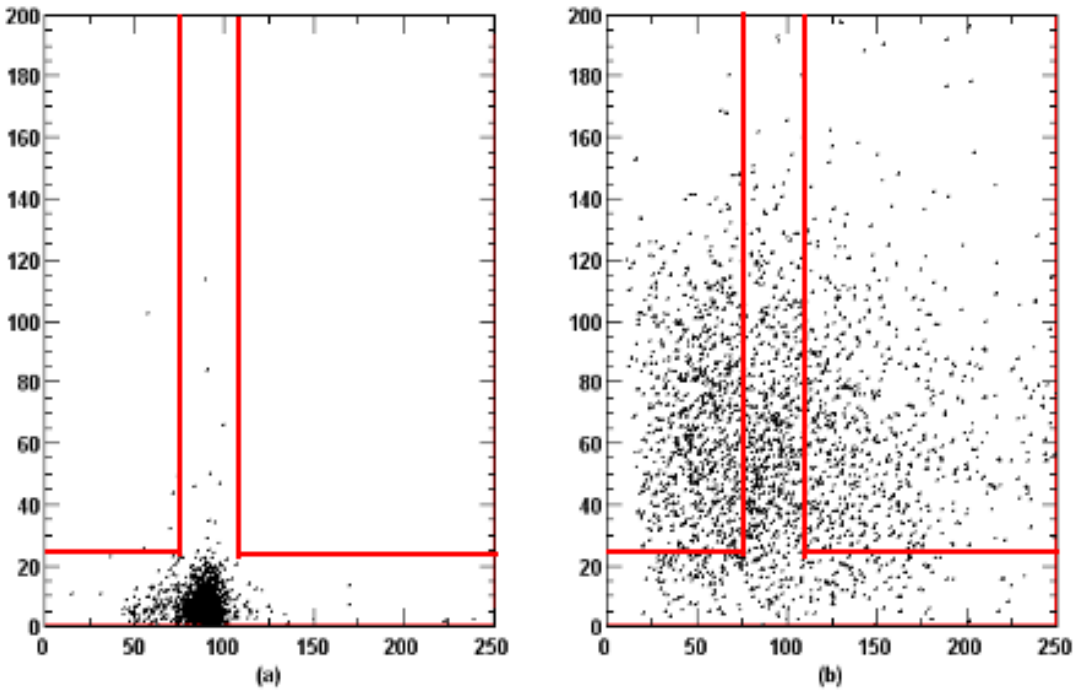

Figure 5: $\not\!\!E_T$ vs. M_{ee} for (a) Z in data and (b) $t\bar{t}\rightarrow ee$ MC.

MC where the τ's are forced to decay to e's μ's. This sample was generated using Alpgen and run through Pythia for fragmentation and gluon radiation. A correction factor of 1.14±0.12 is found using the following equation:

$$C_\tau = \frac{N_{ee}\epsilon_{ee} + N_{e\tau,\tau\tau}\epsilon_\tau}{N_{ee}\epsilon_{ee}},$$

where N_{ee} and ϵ_{ee} are the number of events with both W's decaying to electrons and the efficiency for these events respectively, and $N_{e\tau,\tau\tau}$ and ϵ_τ are the number of $t\bar{t}$'s in which one or both W's decay to τ's which then decay to e's and the efficiency for these events respectively.

6.1 Backgrounds

6.1.1 Physics Backgrounds

The $Z \rightarrow \tau\tau$ background where both taus decay to electrons is estimated from p14.02.00 Alpgen MC run through Pythia for fragmentation and gluon radiation. It was generated in a $Z \rightarrow ll$ inclusive sample where the τ's were forced to decay to electrons and muons. This sample was generated in three dielectron mass regions: 15-60 GeV, 60-130 GeV, and $>$ 130

Cut	Efficiency
Reco, EM Acc (2 EMs,$p_T > 15$ GeV,$\|\eta\| < 1.1$)	0.422 ± 0.005
EM ID cuts	0.793 ± 0.006
2 EMs,$p_T > 20$ GeV	0.905 ± 0.005
Likelihood cut	0.763 ± 0.007
$\not\!\!E_T > 25$ GeV and removal of Z window	0.668 ± 0.009
2 Jet Acc (2 good jets,$p_T > 8$ GeV,$\|\eta\| < 2.5$)	0.810 ± 0.009
2 Jets,$p_T > 20$ GeV	0.891 ± 0.008
$H_T^e > 120$ GeV	0.970 ± 0.005
$\epsilon_{reco*acc*kin*EMID}$	0.108 ± 0.002

Table 2: Efficiencies of kinematic and EM selection cuts on $t\bar{t} \rightarrow$ ee MC.

Cut	Data Efficiency	MC Efficiency	κ
EM ID	0.769 ± 0.011	0.793 ± 0.006	0.969 ± 0.013
Likelihood	0.521 ± 0.115	0.763 ± 0.007	0.683 ± 0.091

Table 3: κ factors relating MC and data efficiencies.

GeV. Its contribution is estimated to be 0.0011±0.0010 events in the same way the expected signal contribution was estimated. This estimate seems low compared to the estimate in [8]. This is probably due to no τ's passing all the selection cuts in the low dielectron mass region, which is where one would expect most of this background to fall. Therefore, the expectation from [8] will be used, scaled to the current luminosity. This gives 0.051±0.029 events. A 20% systematic error is assumed on this number. The WW background was similarly studied using p13.08.00 Pythia MC. The total expected event yield from this background is 0.0071 ± 0.0044 events.

6.1.2 Instrumental Backgrounds

The key background to reject in the dielectron analysis is $Z/\gamma^* \rightarrow ee$ + fake $\not\!\!E_T$. Direct Z/γ^* decays to dielectrons produce no neutrinos, and therefore no real $\not\!\!E_T$. Hence, any such events can only pass the selection criteria if there are resolution effects which cause the measured $\not\!\!E_T$ to fluctuate above the $\not\!\!E_T$ cuts. This can also occur when hot cells or warm regions manifest in the calorimeter. None of these effects are reliably simulated in the MC; hence this background is estimated from the data.

The approach taken is to obtain a sample of events which is similar in terms of kinematics and resolutions to the Z/γ^* events to be rejected. This sample contains di-EM events which pass the signal trigger, have two electrons satisfying only ID=10 or 11, and pass the jet and H_T^e cuts. Note that this 'loose-loose' sample also contains the QCD multijet background where 2 jets fake electrons. The di-EM events in this sample are separated into two mass regions, $M_{ee} < 75$ GeV and $M_{ee} > 105$ GeV, which correspond to the accepted mass regions. It is assumed that, in this 'loose-loose' sample, the signal and physics backgrounds are swamped by Z/γ^* and QCD background. In each mass region,the number of events that fall below the respective $\not\!\!E_T$ cut, N^b_{loose}, and above the $\not\!\!E_T$ cut, N^a_{loose} are counted.

Then, all of the EM selection criteria are applied and the number of events below the $\not\!\!E_T$ cut in each of the three mass regions is counted, assuming that what lies below is still dominated by Z/γ^* and QCD background. If the number of events below in the tight sample is N^b_{tight}, then, the number of background events expected above the $\not\!\!E_T$ cut, N^a_{tight}, can be estimated in each mass region from

$$N^a_{tight} = N^b_{tight} \frac{N^a_{loose}}{N^b_{loose}}.$$

Finally, the estimated Z/γ^* and QCD background which passes all of the selection criteria is

$$N_{Z/\gamma*,QCD} = N^{a_{M<75}}_{tight} + N^{a_{M>105}}_{tight}.$$

This yields 0.513±0.513 $Z/\gamma^* \rightarrow ee$ and QCD background events.

The Z mass window was removed because the $\not\!\!E_T$ distribution has long, non-Gaussian tails causing the $\not\!\!E_T$ fake rate to be considerably higher than in Run I. The electrons and the Z mass are fairly well resolved and understood. However, because the tails in the $\not\!\!E_T$ distribution it is not uncommon for a Z event to have high $\not\!\!E_T$ as shown in Figure 5. Hence, to obtain reasonable

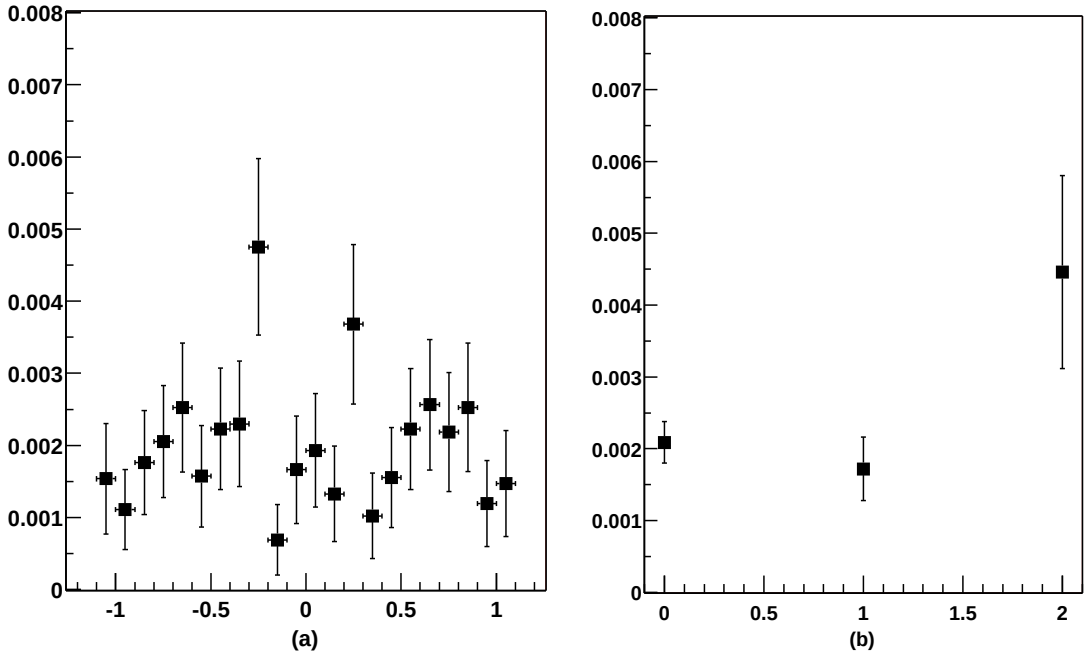

Figure 6: (a)EM fake rate vs η. (b)EM fake rate vs jet multiplicity.

background levels, a $\not\!\!E_T$ cut is no longer be applied in the Z mass window; the resonance must be removed entirely for now.

The final background, W+jets, arises from a jet which fragments or showers such that it appears electron-like. The probability for such a jet to pass the electron ID cuts was measured in a loose di-EM sample selected using the 2EM_HI trigger. Starting with loose (ID=10 or 11) EM objects, with $\not\!\!E_T$ <15 GeV and $M_{ee} < 50$ GeV, the fake rate is defined as the fraction of loose EM objects which survive when tight electron cuts are applied. As a cross check, this fake rate has also been studied using a sample of events passing any muon-only trigger and having at least one L1 EM tower with $E_T > 10$ GeV [8]. The fake rate for EM clusters in events satisfying the L1+L3 requirement in the muon-triggered sample has also been studied [8]. The fake rates are roughly consistent across triggers, and no significant bias is observed for the L3 requirement in comparison to just the L1 selection in the muon-triggered sample. In all cases, the fake rate, f_{em}, is flat in jet multiplicity and in η for $|\eta| < 1.1$ as shown in Figure 6. Fake rates by jet multiplicity can be found in Table 4. Since 2 jets are required for the signal, the fake rate from the 2 jet bin is used.

Furthermore, since the electrons in the signal events are required to be oppositely-charged, fake rates for positrons and electrons can be obtained using the charge distributions of EM objects passing the tight selection cuts. Figure 7 shows that there are nearly equal numbers

# of Jets	f_{em}
0	0.0021 ± 0.0003
1	0.0017 ± 0.0004
2	0.0045 ± 0.0013

Table 4: EM fake rates by jet multiplicity.

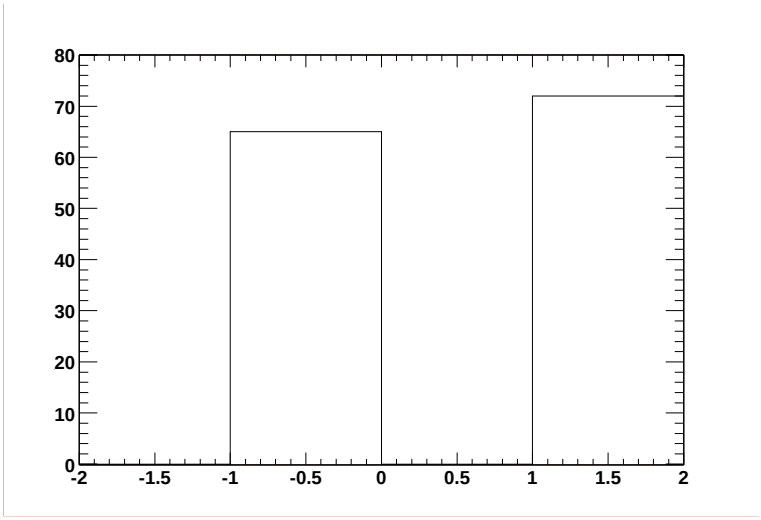

Figure 7: Charge distribution of EM objects passing tight selection.

of positively and negatively charged objects. Thus,

$$f_{em}^{+} = f_{em}^{-} = \frac{f_{em}}{2} = 0.0023 \pm 0.0007 \pm 0.0002.$$

A systematic error is added here to account for the slight difference in charge distribution.

Now, to estimate the W+jets background, events are selected with two EM clusters, one ID=10 or 11 only and one of which passes the tight ID, and all of the other selection criteria. The number of 'loose-tight' events, N_{lt}, is then multiplied by the corresponding $f_{em}^{\pm}$,

$$N_{WQ} = N_{lt} f_{em}^{\pm}.$$

This gives 0.007 ± 0.006 events.

However, there is a probability that the tight electron in the sample is actually a fake; that is, it can happen that a 'tight-loose' event is a QCD event with a jet faking the tight electron. Since the QCD background was counted along with the $Z/\gamma^{*} \rightarrow ee$ background, this

Cut	Data	All	fakes	WW	$Z \to \tau\overline{\tau}$	$t\bar{t}$
$N_{ele}^{P_T>20} \geq 2 + \not\!\!E_T$ cut	5	4.60±0.55	2.81±0.49	0.57±0.12	0.33±0.11	0.89±0.19
$N_{jets} \geq 2$	4	1.69±0.43	0.85±0.40	0.03±0.01	0.09±0.04	0.72±0.16
$N_{jets}^{P_T>20} \geq 2$	3	1.19±0.39	0.49±0.36	0.01±0.00	0.05±0.03	0.64±0.14
$H_T^e > 120$	2	1.19±0.53	0.52±0.51	0.00±0.00	0.05±0.03	0.62±0.14

Table 5: Data and backgrounds at each level of selection, with statistical errors.

contribution must be removed from the W+jets sample. To do this, the number of events with two loose EM objects and all other selection criteria applied, N_{ll}, are counted, and these numbers are multiplied by $f_{em}f_{em}^{\pm}$,

$$N_{QCD} = N_{ll} f_{em} f_{em}^{\pm}.$$

This gives a 0.0020±0.0013 QCD events. The total number of W+jets background events,

$$N_{Wjets} = N_{WQ} - N_{QCD},$$

is then $0.005^{+0.006}_{-0.005}$.

Adding the W+jets background expectation to the $Z/\gamma^* \to ee$ and QCD expectation gives a total fake background expectation of 0.52±0.51 events.

The overall background estimate compared to data at each cut level is summarized in Table 6.1.2.

6.2 Observed Event Yield

When imposing all selection criteria, two events pass all of the cuts. Their run and event numbers are 167194:12104152 and 176692:43130892. The only dielectron event from [8] that survives is the one from run 167194. The other three events have at least one electron which does not pass the likelihood cut. Tables 8 and 9 show the kinematics of the two candidate events, and Figures 8 and 9 show the event displays.

6.3 Cross Section

A summary of systematic uncertainties is presented in Table 6.2. Using these values, a cross section can be obtained. The cross section is

$$\sigma = \frac{N_{obs} - N_{bkg}}{\mathcal{L} BR_{ee} C_\tau \epsilon_{top}},$$

where N_{obs} and N_{bkg} can be found in Table 6.3, $\mathcal{L}$ is the integrated luminosity, and BR_{ee} is 1/81. The signal efficiency,ϵ_{top}, is $0.063 \pm 0.014 \pm 0.009$. This yields a top cross section of

$$\sigma_{p\bar{p}\to t\bar{t}} = 14.96 \ {}^{+20.70}_{-14.96} \ \text{(stat)} \ \text{pb}.$$

	Systematic Uncertainty
PV	2.0%
e_{ID}	5.0%
e_{p_T}	0.4%
$e_{likelihood}$	5.2%
TRK	3.2%
JES	$^{+5.6\%}_{-5.3\%}$
Jet_{ID}	1.4%
Jet res.	8.0%
Trigger	5.0%
Luminosity	10%

Table 6: Summary of systematic uncertainties.

Category	Yield	Stat Err	Sys Err
$Z \to \tau\tau$	0.051	0.029	0.013
WW	0.004	0.003	0.001
Fakes	0.52	0.51	0.07
Total Bkg	0.58	0.51	0.07
Selected Events	2.00	1.41	–

Table 7: Yield summary for $t\bar{t} \to ee$ channel.

Object	p_T (GeV)	η	ϕ
ele1	89.4	0.34	1.86
ele2	30.5	-0.22	0.45
jet1	35.4	0.48	4.58
jet2	25.4	-1.69	5.71
jet3	21.7	-0.06	2.66
MET (GeV)	49.6		
DiEM Mass (GeV)	74.0		

Table 8: Kinematics for event 12104152 in run 167194.

Object	p_T (GeV)	η	ϕ
ele1	38.2	0.75	5.35
ele2	21.6	-0.05	1.22
jet1	54.3	0.53	3.46
jet2	42.2	1.56	1.74
MET (GeV)	25.0		
DiEM Mass (GeV)	55.8		

Table 9: Kinematics for event 43130892 in run 176692.

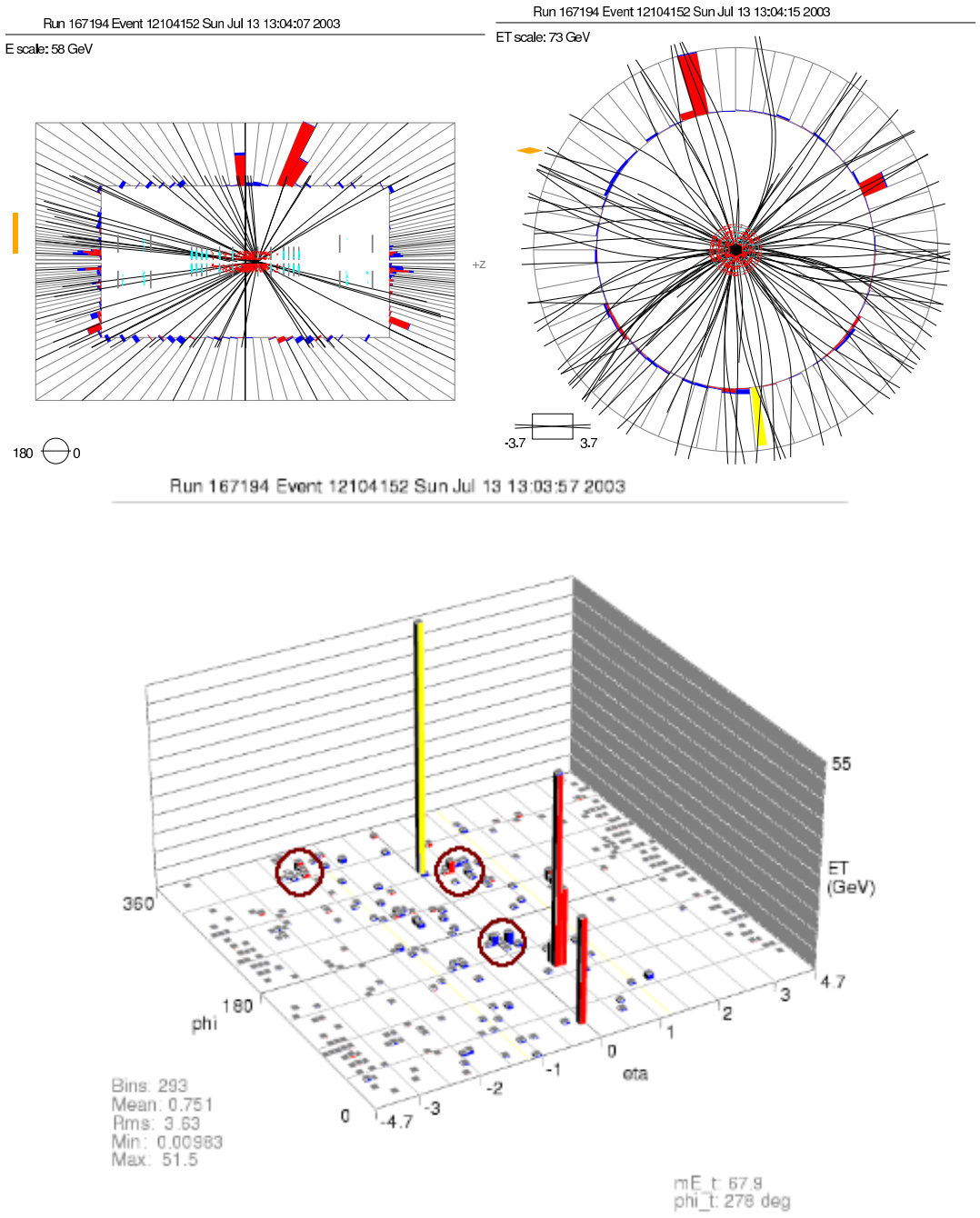

Figure 8: Run 167194 Event 12104152: RZ view (upper right), XY view (upper left), Lego view (lower). Jets are circled in the lego plot.

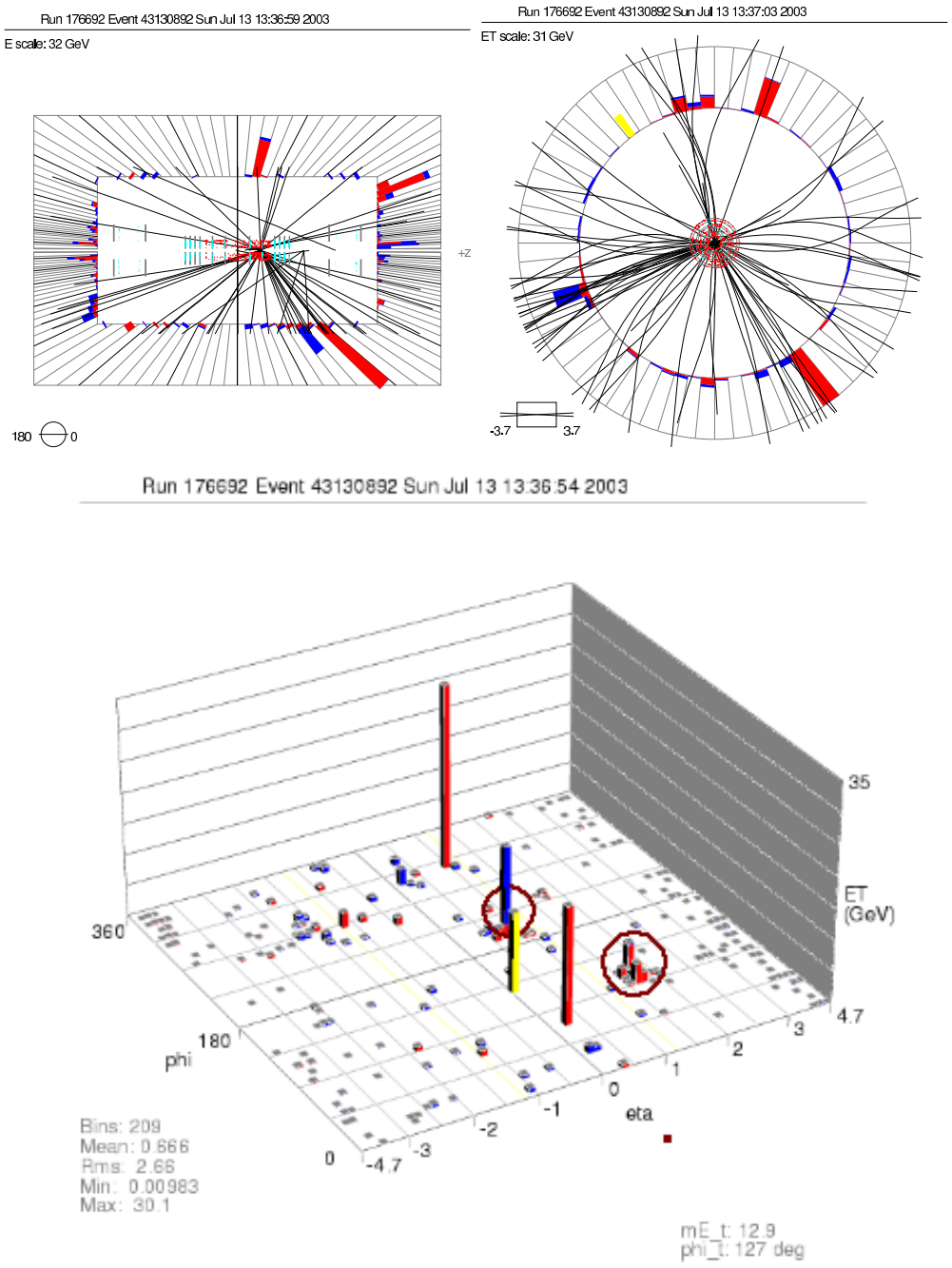

Figure 9: Run 176692 Event 43140892: RZ view (upper right), XY view (upper left), Lego view (lower). Jets are circled in the lego plot.

References

[1] S. Anderson, et al., DØ-Note 4116.

[2] M. Klute, DØ-Note in preparation.

[3] L. Phaf, DØ-Note in preparation.

[4] D. Whiteson and L. Phaf, DØ-Note 4184.

[5] G. Blazey, et al., DØNote 3750.

[6] Jet Certification, v 2.1, http //www-d0.fnal.gov/ ∼d0upgrad/d0_private/software/jetid/certification/v2_0/jetid_p13.html.

[7] R. Demina, et al., DØ-Note 4141.

[8] S. Anderson, et al., DØ-Note 4178.